J Bioenerg Biomembr (2012) 44:399–409
DOI 10.1007/s10863-012-9437-0

Differential distribution of pigment-protein complexes in the Thylakoid membranes of *Synechocystis* 6803

Rachna Agarwal · Gururaj Maralihalli · V. Sudarsan · Sharmistha Dutta Choudhury · Rajesh Kumar Vatsa · Haridas Pal · Michael Melzer · Jayashree Krishna Sainis

Received: 15 December 2011 / Accepted: 26 February 2012 / Published online: 24 May 2012

Abstract Thylakoids in *Synechocystis* 6803, though apparently uniform in appearance in ultrastructure, were found to consist of segments which were functionally dissimilar and had distinct proteomes. These thylakoid segments can be isolated from *Synechocystis* 6803 by successive ultracentrifugation of cell free extracts at 40,000×g (40 k segments), 90,000×g (90 k segments) and 150,000×g (150 k segments). Electron microscopy showed differences in their appearance. 40 k segments looked feathery and fluffy, whereas the 90 k and 150 k thylakoid membrane segments appeared tiny and less fluffy. The absorption spectra showed heterogeneous distribution of pigment-protein complexes in the three types of segments. The photochemical activities of Photosystem I (PSI) and Photosystem II (PSII) showed unequal distributions in 40 k, 90 k and 150 k segments which were substantiated with low temperature fluorescence measurements. The ratio of PSII/PSI fluorescence emission at 77 K (λ_{ex}=435 nm) was highest in 150 k segments indicating higher PSII per unit PSI in these segments. The chlorophyll fluorescence lifetimes in the membranes, determined with a time-correlated single-photon counting technique, could be resolved in three components: τ_1=<40 ps, τ_2=425–900 ps and τ_3=2.4–3.2 ns. The percentage contribution of the fastest component (τ_1) decreased in the order 40 k>90 k>150 k segments whereas that of the other two components showed a reversed trend. These studies indicated differential distribution of pigment-protein complexes in the three membrane segments suggesting heterogeneity in the thylakoids of *Synechocystis* 6803.

Keywords Cyanobacteria · 77K Fluorescence · Heterogeneity · *Synechocystis* 6803 · TCSPC · Thylakoid membranes

Abbreviations

GAPDH	Glyceraldehyde-3-phosphate dehydrogenase
PGK	Phosphoglycerate kinase
PRK	Ribulose-5-phosphate kinase
PS	Photosystem
RPI	Ribose-5-phosphate isomerase
RuBisCO	Ribulose-1, 5-bisphosphate carboxylase/ oxygenase
TCSPC	Time-correlated single-photon counting

Introduction

The light reactions of photosynthesis involve the pigment-protein complexes viz. Photosystem I (PSI) and Photosystem II (PSII) along with the $Cytb_6f$ complex, located in the thylakoid membranes of higher plant chloroplasts and

Electronic supplementary material The online version of this article (doi:10.1007/s10863-012-9437-0) contains supplementary material, which is available to authorized users.

R. Agarwal · G. Maralihalli · J. K. Sainis (✉)
Molecular Biology Division,
Mumbai 400085, India
e-mail: jksainis@barc.gov.in

V. Sudarsan · R. K. Vatsa
Chemistry Division,
Mumbai 400085, India

S. D. Choudhury · H. Pal
Radiation & Photochemistry Division,
Bhabha Atomic Research Centre,
Mumbai 400085, India

M. Melzer
Leibniz Institute of Plant Genetics and Crop Plant Research,
Gatersleben 06466, Germany

prokaryotic cyanobacteria (Wollman et al. 1999). The two photosystems have pigments like carotenoids and chlorophylls (including reaction center chlorophylls) that capture the solar energy leading to abstraction of electrons from water. These electrons, then flow through the photosynthetic electron transport chain in a non-cyclic manner involving both PSII and PSI resulting in the formation of energy rich molecules i.e. NADPH and ATP (Z-scheme) (Hill and Bendall 1960). Alternatively the electrons can be ejected directly from PSI and returned back to it in a cyclic pathway leading only to ATP formation.

Inspite of the assumptions of functional harmony among components of electron transport, heterogeneity in the distribution of PSII and PSI complexes was observed in chloroplasts of higher plants. Heterogeneity in PSII populations having difference in antenna size and membrane localization was shown by Armond and Arntzen (1977). Andreasson et al. (1988) demonstrated heterogeneity in PSI populations in Spinach chloroplasts. PSI is preferentially located in the non appressed stroma lamellae and PSII is present in appressed granal regions in eukaryotic systems (Staehelin and Arntzen 1983; Anderson and Aro 1994). This lateral heterogeneity is considered to minimize the damage due to light stress and manage the excitonic control as the machinery of the two photosystems especially PSII is vulnerable to light stress (Nishiyama et al. 2005).

Although well documented and proven in higher plants, the concept of heterogeneity in thylakoids of cyanobacteria is seldom recognized owing to the absence of visual differences in the ultrastructure of the thylakoids. However, there are a few reports indicating heterogeneity even in the thylakoids of cyanobacteria. Sherman et al. (1994) have reported localization of PSI in the outer thylakoids and PSII in the inner thylakoids of *Synechococcus* 7942 by immuno-gold transmission electron microscopy. In contrast, Vermaas et al. (2008) have shown preferential location of PSI in the inner thylakoids by employing in vivo hyperspectral confocal fluorescence imaging. Kumazaki et al. (2007) have reported higher association of phycobilisome with outer thylakoids using spectral measurement of sub-cellular domains in *Anabaena* PCC 7120. It was shown that the fluorescence intensity ratio between chlorophyll molecules mainly of PSII and phycobilin molecules of phycobilisomes in the thylakoid membranes reduced as the inside of the cells was probed deeper. This was attributable not to the positional dependence of reabsorption or scattering effects, but to the intrinsic changes in the local physiological state of the thylakoid membranes. Recently, Rexroth et al. (2011) have demonstrated heterogeneity in the plasma membrane of *Gloeobacter violaceous*, a cyanobacterium with no thylakoid membranes.

We had observed that the thylakoids from cell free extracts of *Anacystis nidulans* BD-1 (*Synechococcus* spp.) and *Synechocystis* 6803 can be fractionated in three segments sedimenting at 40,000×g, 90,000×g and 150,000×g by ultracentrifugation. A comparative analysis of 40 k, 90 k and 150 k fractions had shown that the 150 k fraction had the highest percentage of the linked activities such as Ribose-5-phosphate+ADP+P_i dependent CO_2 fixation and Ribose-5-phosphate+ATP dependent glyceraldehyde-3-phosphate dehydrogenase activity indicating presence of functional light reaction machinery and five sequential enzymes of the Calvin cycle viz. RPI, PRK, RuBisCO, PGK and GAPDH (Dani and Sainis 2005; Agarwal et al. 2009). Subsequently proteomic analysis also showed that the protein composition of these three membrane segments was different from each other (Agarwal et al. 2010).

In the current investigations, we have studied these three thylakoid segments for their biophysical characters using low temperature and time-resolved fluorescence as well as functional analysis of electron transport properties which suggested differential distribution of pigment-protein complexes in the thylakoids of *Synechocystis* 6803.

Material and methods

Culture growth Culture of *Synechocystis* 6803, obtained from Dr. Wim Vermaas, Arizona State University, was grown in BG-11 medium (Rippka et al. 1979) under continuous white light of intensity 21 W/m^2 and constant temperature of 30 °C. When O.D. at 730 nm of the cell culture was 0.2–0.3, cells were harvested for isolation of thylakoid membranes.

High pressure freezing, freeze-substitution and transmission electron microscopy of the cells of Synechocystis 6803 High pressure freezing of cells in the log phase has been performed as described previously (Agarwal et al. 2009).

Thylakoid membrane isolation and transmission electron microscopy Thylakoid membranes were isolated as described by Murata et al. (1981) with the following modifications. Cells from 2 l culture were harvested, washed and resuspended in 20 ml of membrane isolation buffer (MIB) containing 10 mM Tris–HCl, pH 7.8; 10 mM $MgCl_2$; 50 mM $NaHCO_3$; 1 mM EDTA; 12 mM β Mercaptoethanol and 10 % sucrose containing 3 mg PMSF. The cell-free extracts were prepared by sonication at 4 °C for 50 min in pulse mode. The extract was centrifuged at 8000 rpm (SS34 rotor in Sorvall centrifuge) at 4 °C for 10 min to remove unbroken cell debris. Supernatant was subjected to sequential ultracentrifugation at 40,000×g, 90,000×g and 150,000×g for 1 h each at 4 °C as described previously (Agarwal et al. 2009, 2010). The pellets after each round of centrifugation were resuspended in 0.2–1.0 ml of DCMU (3-(3, 4-dichlorophenyl)-1, 1-dimethylurea) and referred to as 40 k, 90 k and 150 k

membrane segments (fractions). Transmission electron microscopy analysis of the three types of segments has been carried out as described by Agarwal et al. (2009).

Pigment estimation Chlorophyll a estimation was done according to Tandeau de Marsac and Houmard (1988). Briefly, cell pellet was extracted with 90 % methanol for 15 min at RT and centrifuged at 10,000 rpm for 2 min. The chlorophyll a content was calculated from the absorbance of the methanolic extract at 665 nm, using the equation:

$$\mathrm{Chl}\left(\mu\mathrm{g.\,ml^{-1}}\right) = \mathrm{O.D.}_{665\mathrm{nm}} \times 13.9$$

Phycocyanin (PC) and allophycocyanin (AP) were calculated using the simultaneous equations of Bennett and Bogorad (1973) and the extinction coefficients from Bryant et al. (1979) as follows:

$$\mathrm{PC}\left(\mathrm{mg.\,ml^{-1}}\right) = \mathrm{O.D.}_{620\mathrm{nm}} - 0.7 * \mathrm{O.D.}_{650\mathrm{nm}}/7.38$$

$$\mathrm{AP}\left(\mathrm{mg.\,ml^{-1}}\right) = \mathrm{O.D.}_{650\mathrm{nm}} - 0.19 * \mathrm{O.D.}_{620\mathrm{nm}}/5.65$$

Carotenoids were estimated by using the equation given by Santhose et al. (2011) as follows:

$$\mathrm{Carotenoids}\left(\mu\mathrm{g.\,ml^{-1}}\right) = \mathrm{O.D.}_{480\mathrm{nm}} * 100$$

Phycocyanin, Allophycocyanin and carotenoids were determined on equal chlorophyll basis and expressed in terms of percent distribution among the 40 k, 90 k and 150 k thylakoid membrane segments.

Assay of photochemical activities in thylakoid membranes PSI activity was measured polarographically in the three thylakoid membrane segments by following oxygen consumption in light and dark using a Clarke type oxygen electrode and expressed as μMoles O_2 consumed, mg Chl^{-1}, h^{-1}. The membrane pellet was resuspended in MIB. The reaction mixture consisted of membranes containing 3–30 μg chlorophyll in 50 mM Tricine-KOH buffer pH 7.6 having 5 mM $MgCl_2$, 50 mM KCl, 50 μM DCPIP, 2 mM Sodium ascorbate, 2 mM Sodium azide, 5 mM Ammonium Chloride, 5 μM DCMU and 50 μM methyl viologen in a volume of 2 ml. PSII activity was measured spectrophotometrically using Hill's reaction with DCPIP (2, 6-dichlorophenolindophenol) as the electron acceptor and expressed as μMoles DCPIP reduced, mg Chl^{-1} h^{-1}. Thylakoid membranes were resuspended in Tricine-KOH buffer pH 7.6 containing 5 mM $MgCl_2$ and 50 mM KCl. 50 μM DCPIP was added to these membranes and photo reduction of DCPIP at 600 nm was followed for 2 min (ε=19.1 mM cm^{-1}).

Time-resolved fluorescence measurements An IBH instrument, based on the time-correlated single-photon-counting (TCSPC) principle, was used for the time-resolved fluorescence measurements. Membranes corresponding to 5 μg chlorophyll were resuspended in MIB (Membrane isolation buffer) to a final volume of 1 ml and the fluorescence decay measurements were performed at RT. A 445 nm diode laser (~100 ps pulse width, 1 MHz repetition rate) was used as the excitation source and a MCP-PMT (Micro-channel plate photomultiplier tube) based detection module was used for the measurement of the fluorescence decays. Emission wavelength was 685 nm. All the fluorescence decays were collected at magic angle (54.7°) with respect to the vertically polarized excitation light, to avoid the effect of rotational depolarization on the measured fluorescence lifetimes. The DAS-6 software from IBH was used for the deconvolution analysis of the observed decays, considering multi-exponential decay functions. With this analysis, the shortest fluorescence lifetime measurable using the present TCSPC instrument is ~40 ps. The quality of the fits and consequently the multi-exponential natures of the decays were judged by the reduced chi-square (χ^2) values and the distribution of the weighted residuals among the data channels. For a good fit, the χ^2 value was close to unity and the weighted residuals were distributed randomly around zero among the data channels.

Low temperature (77 K) fluorescence measurements Emission and excitation spectra were recorded for all the samples with an Edinburgh Instruments' FLSP 920 system attached with a 450 W Xe lamp as the excitation source and red sensitive PMT as the detector. For 77 K experiments, a liquid nitrogen cryostat supplied by Oxford Instruments was used. The emission spectra were recorded with a resolution of 3 nm and all of them were corrected for the detector responses. The chlorophyll concentration was 5 μg chlorophyll, ml^{-1} in cases of all the samples during measurements.

Results

Ultracentrifugation of the cell free extracts prepared by sonication of cells of *Synechococcus spp*. (earlier called as *Anacystis nidulans* BD1) and *Synechocystis* 6803 yielded three thylakoid fractions sedimenting at 40,000×g, 90,000×g and 150,000×g. Such fractions were also obtained from these cells if the cells were broken by French press (unpublished) suggesting the presence of definite segments of thylakoids in these cyanobacteria. These three fractions had shown biochemical and proteomic differences among them (Dani and Sainis 2005; Agarwal et al. 2009, 2010). The present study was aimed at exploring the differences in biophysical properties of these three segments of the thylakoid membranes, namely 40 k, 90 k and 150 k, obtained from the cell free extracts of the unicellular cyanobacterium *Synechocystis* 6803.

Electron Microscopy of *Synechocystis* 6803 cells and the three thylakoid segments

Figure 1 (a–d) shows the electron micrographs of *Synechocystis* cells and the three thylakoid segments isolated from its cell free extracts. *Synechocystis* 6803 showed typical ultrastructure with spherical cells having parallel sheets of thylakoids which are attached to the plasma membrane at certain regions giving them a curtain like appearance. In contrast to the homogenous structure of thylakoids in *Synechocytsis* cells (Fig. 1a), the three membrane segments obtained by differential ultracentrifugation showed distinct differences. 40 k segments appeared more feathery and fluffy as compared to 90 k segments (Fig. 1b and c). The 150 k segments were considerably less fuzzy with tinier fragments (Fig. 1d). This suggested that there are differences in the sizes and appearance of the thylakoid segments settling at 40,000×g, 90,000×g and 150,000×g.

Absorption spectra of *Synechocystis* cells and the three thylakoid segments

To understand the differences in the pigment-protein complexes, the absorption spectra of the three thylakoid membrane segments along with the whole cells were recorded on an equal chlorophyll basis (Fig. 2). The observed absorption spectra were deconvoluted using a Microcal Origin peak fitting module to resolve the absorption peaks. The absorption spectrum of the whole cells showed two peaks corresponding to chlorophylls at 436 nm and ~681 nm respectively, a peak at 512 nm for carotenoids and two peaks at ~600 nm and 630 nm for phycobilisomes absorption (Fig. 2a). An expected 485 nm carotenoid peak, however, could not be resolved in the case of the absorption spectrum for the whole cells. The absorption spectra for the three thylakoid fractions showed most prominent peaks at 436 nm and 678 nm for chlorophyll a, 600 nm and 630 nm for phycobilisomes and less prominent peaks at ~485 nm and 512 nm for carotenoids (Fig. 2b–d). The absorption spectrum of the 150 k segments (Fig. 2d) was essentially similar to the absorption spectrum obtained by Li et al. (2001) for phycobilisomes thylakoid membrane complexes of *Spirulina platensis*. On an equal chlorophyll basis, the 150 k segments showed much higher phycobilisome specific absorption at 630 nm indicating heterogeneous distribution of these pigment-protein complexes in the three thylakoid segments.

Since the absorption spectra revealed distinct differences in the content of phycobilisome in the three segments, we carried out quantitation (represented as percent distribution) of various components of phycobilsomes i.e., phycocyanin and allophycocyanin as well as carotenoids in these thylakoid segments on an equal chlorophyll basis (Fig. 3). The results showed that although the amount of carotenoids is fairly similar among the three segments, the content of phycocyanin and allophycocyanin is much higher in the 150 k fraction than in the 40 k and 90 k

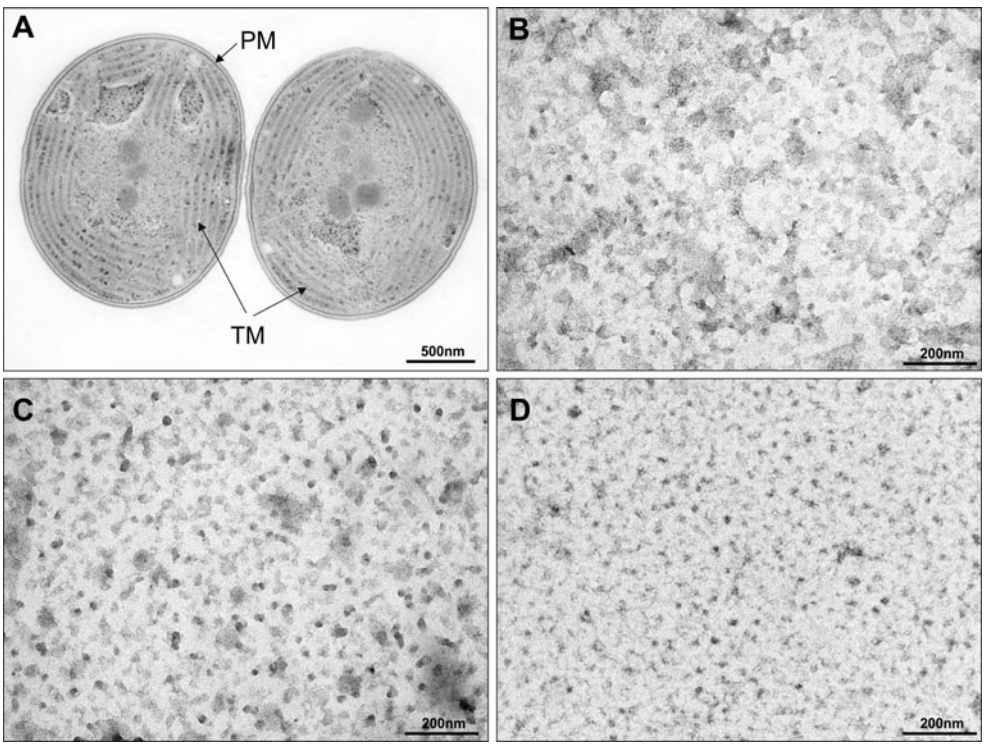

Fig. 1 Transmission Electron Micrographs of *Synechocystis* 6803 cells and thylakoid membrane segments. The whole cells and the thylakoid membrane segments were processed for transmission electron microscopy as described in material and methods. (**a**) Section of a whole cell of *Synechocystis* 6803 (**b**) 40 k segments (**c**) 90 k segments and (**d**) 150 k segments. *TM* thylakoid membrane, *PM* plasma membrane

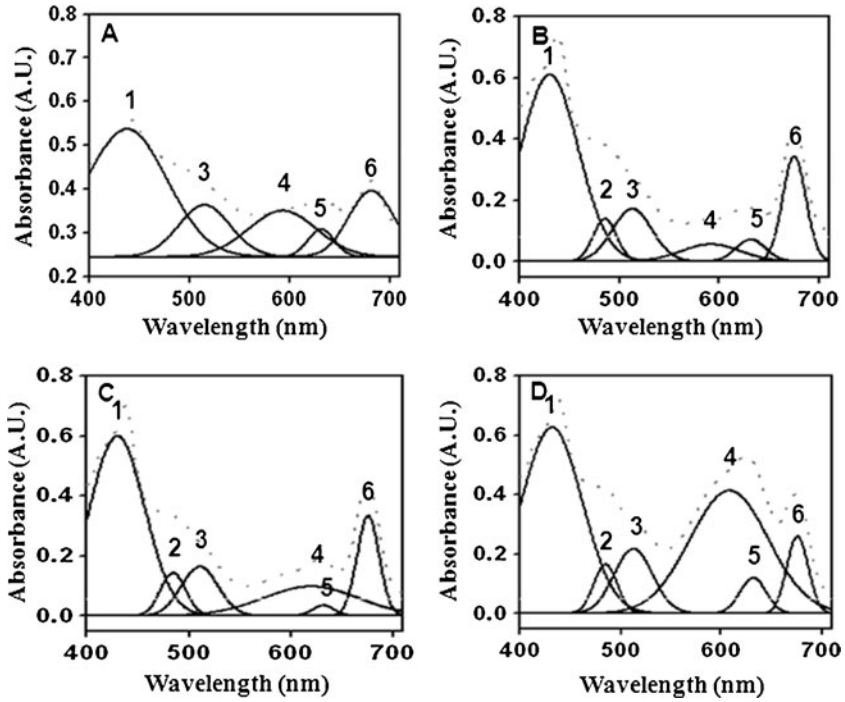

Fig. 2 Absorption spectra of whole cells, 40 k, 90 k and 150 k thylakoid membrane segments from *Synechocystis* 6803. The thylakoid membrane segments from *Synechocystis* 6803 were isolated as described in material and methods, resuspended in buffer and the absorption spectra were recorded on an equal chlorophyll basis. The peaks were deconvoluted using Microcal Origin 5.0 peak fitting module. (**a**) Whole cells (**b**) 40 k segments (**c**) 90 k segments (**d**) 150 k segments. Raw data: Dotted gray line; Fitted spectra: Black lines. The chlorophylls absorb at 436 and 678 nm (Peaks 1 and 6), Carotenoids absorb at 485 nm and 512 nm (Peaks 2 and 3) and phycobilisomes absorb at 600 and 630 nm (peaks 4 and 5). Chlorophylls in whole cells show a peak around 681. The 485 nm carotenoid peak, however, is not resolved in the case of whole cells

fractions on an equal chlorophyll basis (Fig. 3). Moreover, the ratio of absolute values of phycocyanin to allophycocyanin also increased in the order of 40 k<90 k<150 k on an equal chlorophyll basis (0.37: 0.43: 0.91).

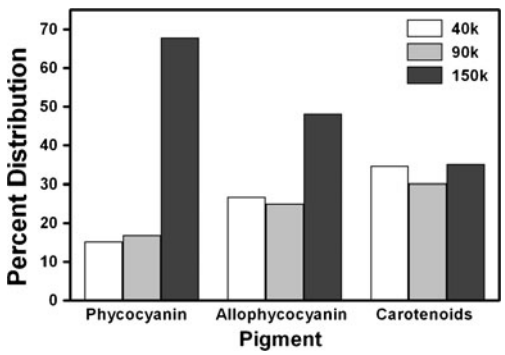

Fig. 3 The distribution of phycocyanin, allophycocyanin and carotenoids among 40 k, 90 k and 150 k thylakoid membrane segments from *Synechocystis* 6803. The thylakoid membrane segments were isolated as described in material and methods and the phycocyanin, allophycocyanin and carotenoids pigments were estimated on equal chlorophyll basis and represented as percent distribution. White column: 40 k segments, Gray column: 90 k Segments, Black Column: 150 k segments

Distribution of PSII and PSI activities in the three thylakoid segments

Light absorption by the pigments ultimately leads to the photochemical light reactions. As there were distinct differences in the chlorophyll (Agarwal et al. 2009) and the phycocyanin-allophycocyanin contents on an equal chlorophyll basis in the three fractions, we studied the distribution of photosystem I (PSI) and photosystem II (PSII) activities in these three thylakoid membrane segments. PSI activity was determined by monitoring oxygen consumption and PSII activity was determined following DCPIP reduction as described in the material and methods section. Table 1 shows the distribution of the total activities and specific activities on an equal chlorophyll basis for PSI and PSII in the three types of the membrane segments. Interestingly, the distribution of total activities showed a trend. 40 k segments had the highest percentage of PSI activity followed by 90 k and 150 k segments whereas 150 k segments showed the highest percentage of PSII activity followed by 90 k and 40 k segments (Table 1). Among the three segments, the 150 k segments had the highest specific activity of PSI (1146.2±117.5 μMoles O_2 consumed, mg Chl^{-1}, h^{-1}) and PSII (614.8±36.4 μMoles DCPIP

Table 1 Distribution of Photosystem I and Photosystem II activities in 40 k, 90 k and 150 k thylakoid membrane segments of *Synechocystis* 6803

Membrane segment	PSI activity		PSII activity	
	Specific activity	Total activity % distribution	Specific activity	Total activity % distribution
40 k	677.7±21.7	66.0	16.2±2.1	12.4
90 k	665.3±47.7	21.8	130.8±7.9	33.8
150 k	1146.2±117.5	12.1	614.8±36.4	53.9

Thylakoid membrane segments were obtained from the cell free extracts of *Synechocystis* 6803 as described in material and methods. PSI activity was determined polarographically following O_2 consumption and expressed as μMoles O_2 consumed mg Chl^{-1}, h^{-1}. PSII activity was determined spectrophotometrically following DCPIP reduction and expressed as μMoles DCPIP reduced, mg Chl^{-1} h^{-1}. Values represent mean±SE (n=3)

reduced, mg Chl^{-1} h^{-1}). The specific activity of PSI was similar in 40 k and 90 k segments (677.7±21.7 and 665.3±47.7 μMoles O_2 consumed, mg Chl^{-1}, h^{-1}), but 90 k segments showed a higher specific activity of PSII (130.8±7.9 μMoles DCPIP reduced, mg Chl^{-1} h^{-1}) as compared to 40 k segments (16.2±2.1 μMoles DCPIP reduced, mg Chl^{-1} h^{-1}). The specific activities have been represented on an equal chlorophyll basis. The ratios of PSII/PSI specific activities were 0.024, 0.197 and 0.536 for 40 k, 90 k and 150 k segments, respectively. Since 150 k segments had higher specific activity of PSI and PSII as compared to 40 k and 90 k segments, the data suggested that 40 k and 90 k segments might have partially assembled or dysfunctional complexes in higher amounts in comparison to 150 k segments. The results pointed to heterogeneity among the functional components of electron transport in the three segments. PSII is known to be damaged and repaired continuously in photosynthetic organisms (Nishiyama et al. 2005) and the three segments may have distinct roles in repair and biogenesis of the two photosystems, especially PSII.

Low temperature fluorescence studies of *Synechocystis* cells and the three thylakoid segments

The differential distribution of PSII and PSI activity was substantiated by low temperature (77 K) fluorescence emission spectra shown in Figs. 4 and 5. Fluorescence of various pigment molecules is a measure of the excited electronic states that results from the absorption of light. It is also an indirect measure of the efficiency of the photoactivation process (Karukstis and Sauer 1983). The chlorophyll molecules in the two photosystems i.e. PSI and PSII and various subunits of phycobilisomes have characteristic excitation and emission wavelengths. The relative amount of the two photosystems can be estimated by fluorescence emission spectroscopy (Fuhrmann et al. 2009). PSII and phycobilisomes fluorescence can be monitored at room temperature. However, owing to its fast kinetics, PSI fluorescence can only be detected at 77 K (Trissl and Wilhelm 1993). 77 K fluorescence analysis of the three thylakoid segments i.e., 40 k, 90 k and 150 k segments was carried out on an equal chlorophyll basis. The emission spectra were recorded at an excitation wavelength for Chlorophyll a at 435 nm (Fig. 4) and for Phycobilisomes at 540 nm (Fig. 5). The excitation at 435 nm gave rise to three distinct peaks around ~650 nm (Phycobilisomes), ~685 nm (PSII) and ~721 nm (PSI) (Fig. 4). On an equal chlorophyll basis, the ratio of PSII/PSI fluorescence emission increased in the order 40 k<90 k<150 k segments (0.10:0.11:0.28:: 40 k:90 k:150 k) indicating a higher amount of PSII complexes per PSI complex in 150 k segments (Table 2). These results support our earlier data on unequal distribution of biochemical activities of PSI and PSII between the three segments where in PSII activity was maximally detected in 150 k segments. In cyanobacteria, excitation at 435 nm normally yields two emission peaks at 685 nm and 695 nm corresponding to PSII and a variable peak between 700 and 735 nm for PSI (Fuhrmann et al. 2009). However, in the present study only two distinct photosystem specific peaks were observed at 685 nm and 721 nm, respectively. Noticeably, the emission spectrum of the whole cells after excitation at 435 nm also yielded emission peaks at ~650 nm (Phycobilisomes), ~685 nm (PSII) and ~721 nm (PSI), as that of the thylakoid membrane segments (Supplementary data online Fig. 1a).

Excitation of phycobilisomes at 540 nm yielded three emission peaks at ~650 nm, ~677 nm and ~721 nm, corresponding to phycobilisomes, terminal emitter of phycobilisomes and PSI respectively (Fig. 5). The amount of fluorescence emission at all the three wavelengths was much higher for 150 k segments in comparison to the other two segments. This is because 150 k segments have a much higher amount of phycobilisomes in comparison to the other two segments on an equal chlorophyll basis (Agarwal et al. 2009, see also Fig. 2d). The emission at 721 nm after excitation at 540 nm indicated some energy transfer from phycobilisomes to chlorophylls of PSI. It may be noted that such energy transfer was also observed in the whole cells (Supplementary data online Fig. 1b). In isolated thylakoids such transfer is rarely observed (Mullineaux 2008), except in some cases where thylakoids are isolated in high salt containing

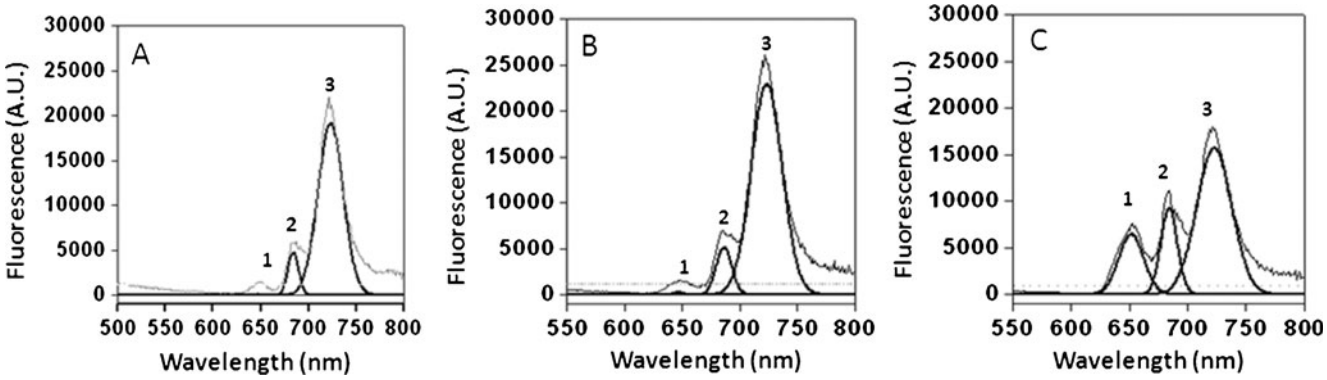

Fig. 4 77K Fluorescence emission spectra of the 40 k, 90 k and 150 k thylakoid membrane segments from *Synechocystis* 6803 recorded with excitation at 435 nm. Fluorescence emission spectra at 77 K were recorded on an equal chlorophyll basis for the three thylakoid segments resuspended in buffer with excitation at 435 nm. (**a**) 40 k segments (**b**) 90 k segments (**c**) 150 k segments. The spectra obtained were corrected for photomultiplier tube response in the red region. The raw spectra obtained were fit by applying a Gaussian deconvolution program. Three different peaks were obtained for all the three segments. Peak 1: ~ 650 nm (Phycobilisomes), Peak: 2~685 nm (PSII), Peak 3: ~721 nm (PSI). Raw data: Gray Line; Fitted spectra: Black line

buffers (Katoh and Gantt 1979). In our thylakoids which were obtained in native conditions, without use of any detergents, the phycobilisomes obtained with the thylakoid segments were probably still energetically coupled with PSI in all the three segments as phycobilisome specific absorption gave emission specific for PSI. Although at 540 nm some amount of direct excitation might also occur for PSI, but as the experiment was conducted on an equal chlorophyll basis, the emission should be the same for all the three membrane segments. Rather it should be less for 150 k segments as can be seen in Fig. 5c where the peak at 721 nm is smaller in 150 k segments in comparison to 40 k and 90 k segments. On the contrary, the ratios of the areas under the curves for emission at 721 nm (Excitation wavelength 540 nm) were approximately 1: 2.5: 60 for 40 k: 90 k: 150 k segments, respectively, which are suggestive of higher energetic coupling of phycobilisomes with thylakoids in 150 k segments in comparison to the other two segments.

Normally phycobilisomes are minimally excited at 435 nm. The peak appearing at 650 nm (after excitation at 435 nm) corresponding to phycobilisome specific emission which is extremely prominent in 150 k segments (Fig. 4) may be arising as a result of minimal phycobilisome excitation at 435 nm and less likely due to back transfer of electrons, a phenomenon described by Li et al. (2001). Its extreme prominence in 150 k segments may be due to a much higher amount of phycobilisomes in these segments in comparison to 40 k and 90 k segments on an equal chlorophyll basis as seen in the absorbtion spectrum (Fig. 2d). A similar peak at 650 nm was also observed in whole cells fluorescence emission spectrum upon excitation with 435 nm (Supplementary data online Fig. 1a).

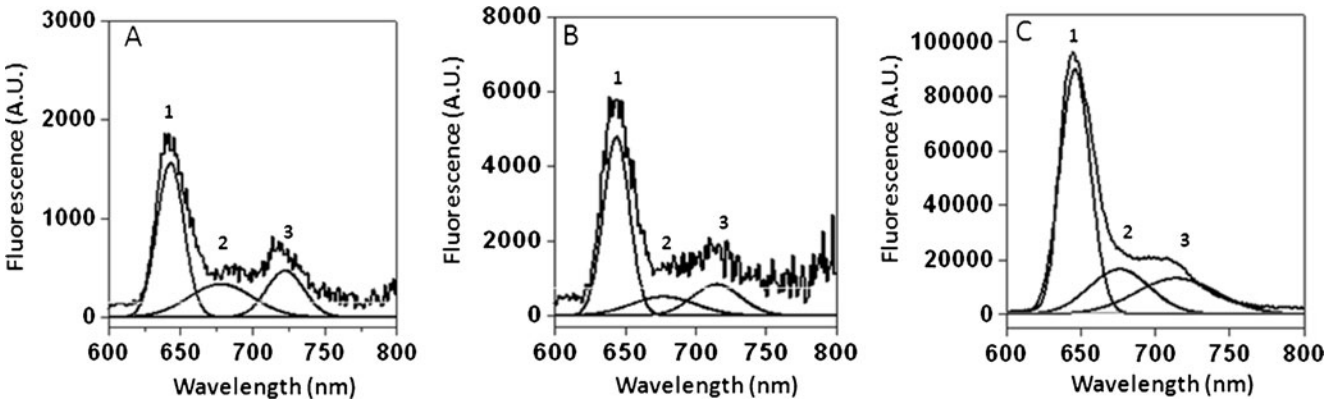

Fig. 5 Fluorescence emission spectra of the 40 k, 90 k and 150 k thylakoid membrane segment from *Synechocystis* 6803 recorded with excitation at 540 nm. Fluorescence emission spectra at 77 K were recorded on an equal chlorophyll basis for the three thylakoid segments resuspended in buffer with excitation at 540 nm. (**a**) 40 k segments (**b**) 90 k segments (**c**) 150 k segments. The spectra obtained were corrected for photomultiplier tube response in the red region. The raw spectra obtained were fit by applying a Gaussian deconvolution program. Three different peaks were obtained for all the three segments. Peak 1: ~650 nm (Phycobilisomes), Peak: 2~677 nm (Terminal emitter of phycobilisomes), Peak 3:~721 nm (PSI). Raw data: Wavy Line; Fit spectra: Smooth line

Table 2 Ratio of fluorescence emission of PSII/PSI for 40 k, 90 k and 150 k thylakoid membrane segments of *Synechocystis* 6803 at 77 K after excitation at 435 nm

Membrane segment	Ratio emission 685 nm/Emission 721 nm (PSII/PSI)
40 k	0.10
90 k	0.11
150 k	0.28

The thylakoid membrane segments were resuspended in buffer and excited at 435 nm (on equal chlorophyll basis). Fluorescence emission spectra were recorded between 550 and 800 nm at 77 K. The raw spectra obtained were fit by applying a Gaussian deconvolution program and the fluorescence yield of emission at 685 nm and 721 nm was calculated as respective areas under the peaks

To confirm the observation of energetic coupling of phycobilisomes to PSI, the excitation spectra were recorded at the emission wavelength of 650 nm (Phycobilisomes) and 721 nm (PSI) (Figs. 6 & 7). The excitation spectra (Fig. 6) for emission at 650 nm (Phycobilisomes) showed two prominent peaks around, λ_{Ex} ~600 nm and λ_{Ex} ~630 nm (Phycocyanin). Since phycobilisomes are higher in 150 k segments, the peak intensity for phyocobilisome specific excitation spectrum was highest in these segments. The excitation spectra were also recorded at PSI specific emission (721 nm) (Fig. 7). The excitation spectra showed peaks at ~600 nm, ~630 nm and ~675 nm specific to various components of phycobilisomes (as seen in emission 650, excitation spectrum, Fig. 6) beside excitation in the blue region of the spectrum (436 nm) which is specific for chlorophyll a. The intensity of emission was higher in 150 k segments as compared to other segments. This confirmed the earlier observation that phycobilisomes are functionally associated with PSI, i.e., they are absorbing light energy and are feeding it to PSI for the actual photochemistry indicating that the phycobilisomes are in state II. The state of the phycobilisomes refers to their attachment to a particular photosystem under a given set of conditions. They are said to be in State I and State II if they are attached to PSII and PSI, respectively. In the present study no appreciable discernible emission peak was observed at either 685 nm or 695 nm after excitation at 540 nm that could be assigned to emission from PSII. Rather a peak at ~675 nm was seen in all the thylakoid segments that conformed to the wavelength for emission from the terminal emitter of phycobilisomes. Since a prominent emission peak at 721 nm was obtained after excitation at 540 nm, it appears that the phycobilisomes were in state II. Existence of the phycobilisomes in state II was also confirmed with excitation spectrum data on the whole cells (emission at 650 nm and 721 nm) where peaks corresponding to phycobilisome specific excitation were observed at ~600 nm, ~630 nm and ~675 nm respectively (Supplementary data online Fig. 2a, b)

Fluorescence life time measurements in the three thylakoid segments

In order to understand the differences in the chlorophyll excited state relaxation process among the three thylakoid membrane segments, chlorophyll fluorescence lifetime measurements were carried out using the time-correlated single-photon-counting technique. Fluorescence lifetime is the time spent by a fluorophore in the excited state before relaxing down to the ground state (Lakowicz 2006). The shorter lifetimes of a fluorphore indicate higher quenching of the excited states. The fluorescence arising from a simple chlorophyll solution is homogeneous in nature. However, in vivo, the situation is very complex and multi-exponential due to the presence of various quenching mechanisms. It is generally assumed that different chlorophyll fluorescence components arise from different portions of the antenna pigment or from the reaction center themselves (Karukstis and Sauer 1983). Most of the previous studies have reported three or more chlorophyll fluorescence lifetime components (Keuper and Sauer 1989). The ultrafast component <15 ps was ascribed to fast reversible excitation equilibration between antennae

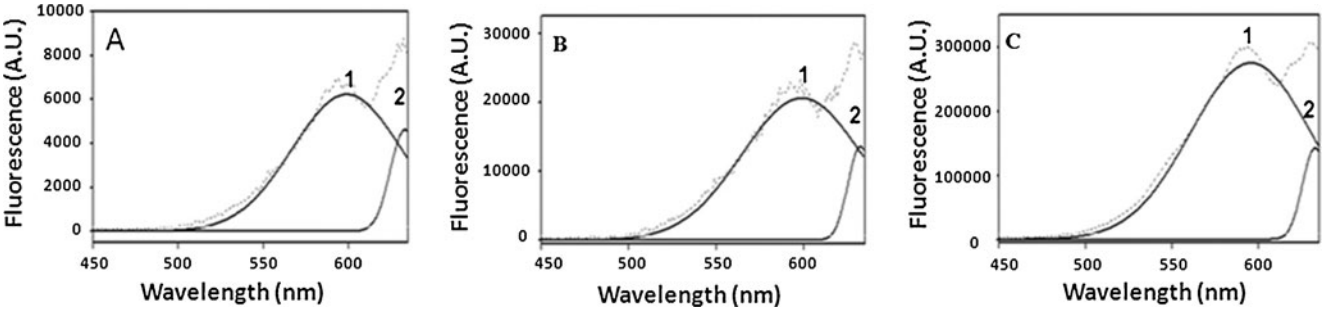

Fig. 6 Fluorescence excitation spectrum of the 40 k, 90 k and 150 k thylakoid membrane segments from *Synechocystis* 6803 recorded at emission wavelength 650 nm for phycobilisomes. 77 K fluorescence excitation spectra were recorded at 650 nm for the three thylakoid segments resuspended in buffer on equal chlorophyll basis. (**a**) 40 k segments (**b**) 90 k segments (**c**) 150 k segments. The raw spectra obtained were fit by applying a Gaussian deconvolution program. Peak1: ~ 600 nm and Peak2: 630 nm corresponding to various components of phycobilisomes. Raw data: Dotted gray line; Fit spectra: Black smooth lines

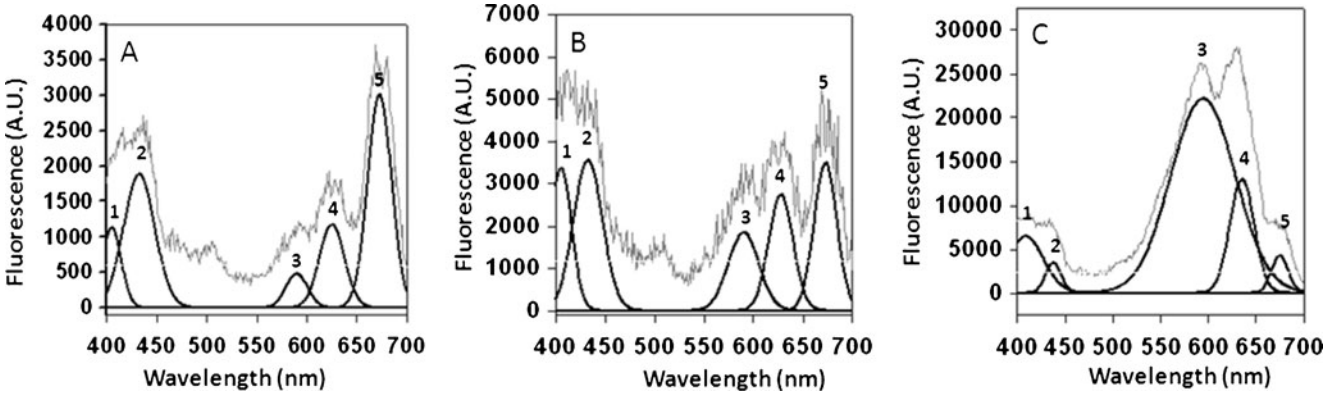

Fig. 7 Fluorescence excitation spectra of the 40 k, 90 k and 150 k thylakoid membrane segments from *Synechocystis* 6803 recorded at emission wavelength 721 nm for PSI. 77 K fluorescence excitation spectra were recorded on an equal chlorophyll basis at 721 nm. (**a**) 40 k segments (**b**) 90 k segments (**c**) 150 k segments. The raw spectra obtained were fit by applying a Gaussian deconvolution program. Peak1: 436 nm (chlorophyll a), Peak2: ~600 nm, Peak3: ~630 nm, Peak4: ~675 nm (various components of phycobilisomes). Raw data: Dotted gray line; Fit spectra: Black smooth lines

and reaction centers (Holzwarth 1990; McCauley et al. 1990). A middle component of 100–740 ps has been ascribed to various forms of PSII in the open or closed state (Holzwarth 1990). The longest component of 1–2 ns has been suggested to be due to closed reaction centers (results from initial charge separation followed by the recombination in the blocked reaction centers) (Karukstis and Sauer 1983). In the present study, chlorophyll fluorescence lifetimes were measured by a diode based laser excitation at 440 nm and monitoring emission at 685 nm (PSII) at room temperature using a MCP-PMT detector. For all the membrane segments, the lifetimes could be resolved into three components: τ_1=<40 ps, τ_2=425–900 ps and τ_3=2.4–3.2 ns (Table 3). The life time values of τ_2 and τ_3 were higher in 150 k segments as compared to 40 k and 90 k segments. The fastest component (τ_1) attributable to excitation equilibration of reaction center chlorophyll contributed almost 100 % for 40 k segments but decreased to 87.2 % for 90 k segments and ~42 % for 150 k segments. A reverse trend was observed for the other two components i.e., the contribution of the middle (τ_2) and the slow component (τ_3) increased in the order 40 k<90 k<150 k segments. These results are consistent with the model discussed in the literature in which the fluorescence of the fast and the middle components are attributed to the excitation lost in transit to the PSII reaction center from different antenna pigments (Karukstis and Sauer 1983). A contribution from the antenna of PSI having fast fluorescence kinetics may also be present in the τ_1 component observed in the present study. Following this literature report, the slow component is attributed to the fluorescence following charge separation in a closed reaction center. The higher contribution of the shorter (τ_1) lifetime component in 40 k segments may thus be due to unfruitful loss of antenna chlorophyll excitation energy during tansit to PSII. Alternatively, there may be some contribution of fluorescence from the PSI as proposed by Magde et al. (1982). Noticeably, 40 k segments have higher specific activity of PSI than PSII. The lifetime values (τ_2 and τ_3 components) of the excited states increased from 90 k to 150 k segments indicating closure of the traps. It is known that inhibition of photochemistry at the level of PSII by addition of inhibitors like DCMU and hydroxylamine that leads to closure of the traps, results in an increase in the fluoresecnce life time of middle and slow components (Magde et al. 1982). An alternate plausible explanation may be the higher amount of functional PSI in 40 k and 90 k segments in comparison to PSII as shown by activity measurements and

Table 3 Chlorophyll fluorescence lifetime measurements of 40 k, 90 k and 150 k thylakoid membrane segments from *Synechocystis* 6803 after excitation at 440 nm

S.No.	Membrane segment	λ_{Ex} (nm)	λ_{Em} (nm)	τ_1 (ps)	Contribution %	τ_2 (ps)	Contribution %	τ_3 (ns)	Contribution %	χ^2	Slit width (nm)
1	40 k	445	685	<40 ps	99.93	425	Negligible	2.43	Negligible	0.92	16
2	90 k	445	685	<40 ps	87.21	413	5.31	2.39	7.48	1.12	16
3	150 k	445	685	<40 ps	42.20	900	26.80	3.18	31.00	1.10	16

The thylakoid membrane segments, resuspended in buffer, were excited at 440 nm (on equal chlorophyll basis) and chlorophyll fluorescence decay measurements were recorded at 685 nm at room temperature. The DAS-6 software from IBH was used for the deconvolution analysis of the observed decays, considering multi-exponential decay functions

77 K fluorescence analysis. As per the Z-scheme of photosynthetic electron transport, electrons are transported from PSII to PSI through intermediate electron acceptors and donors. Most prominently, Q_A gets converted to Q_B (reduced plastoquinol) on accepting the electrons from PSII which then transfers the electrons to PSI. An accumulation of reduced pastoquinol pool is known to inhibit PSII photochemistry. In 40 k segments, PSI, the final acceptor of electrons from PSII, is available in much higher quantities than PSII which may be the reason for efficient electron abstraction from Q_B and therefore, these centers remain open for a longer time. But in case of 150 k segments the ratio of PSII to PSI is higher. As a result, PSI may get saturated faster which would result in Q_B remaining reduced and thus leading to removal of excitation energy from PSII as fluorescence with longer lifetimes. Noticeably, no exogenous ferredoxins or other electron acceptors have been provided in this study which can empty the PSI.

We also carried out Blue Native PAGE of the three thylakoid segments on equal protein basis (Supplementary data online Fig. 3). Our results with Blue native PAGE have shown that 40 k and 90 k membranes have a higher content of PSI whereas 150 k segments have a higher amount of PSII. Moreover 40 k and 90 k segments also have low molecular weight PSII (beside high molecular weight PSII) which might correspond to either monomers or partially assembeled supercomplexes, whereas 150 k has only PSII corresponding to complete monomer or a dimer (Watanabe et al. 2009; Takahashi et al. 2009). Although, it is not possible to comment on the exact molecular weight of proteins on native gels, the PSII bands obtained in our study may belong to differentially assembled complexes.

Discussion

The present study indicated unequal distribution of pigment-protein supercomplexes such as phycobilisomes, PSI and PSII in the three thylakoid membrane fragments termed as 40 k, 90 k and 150 k segments suggesting heterogeneity in these three thylakoid segments of *Synechocystis* 6803. If one considers a homogenous distribution of PSI and PSII in the cyanobacterial thylakoids, then there should not be any differential distribution of these supercomplexes in the membranes of different sizes, i.e. if a membrane of size 10X is harboring 30PSI and 10PSII supercomplexes (3:1) then a membrane of size 1X should have 3PSI and 1PSII supercomplexes. Nonetheless, the results presented here both in terms of biochemical activity data and low tempertaure fluorescence data, reveal selective enrichment of PSII over PSI in 150 k segments as compared to 40 k to 90 k segments. Absorption and fluorescence spectra also indicated a higher proportion of phycobilisomes and their energetic coupling with PSI in 150 k segments. The 77 K fluorescence studies revealed that the higher efficiency of linked light–dark reactions in 150 k segments (Agarwal et al.. 2009) may be due to the presence of equitable amounts of PSI and PSII to operate in a non-cyclic manner leading to the formation of ATP and NADPH required for carbon dioxide fixation besides actual presence of Calvin cycle enzymes (Agarwal et al. 2009, 2010). The other two segments may have only cyclic photophosphorylation operating due to predominance of PSI. The results of chlorophyll fluorescence lifetime measurements also showed existence of heterogeneity in the photosystems present in the three membrane segments. The overall picture projected by the combination of these results conforms to the existence of heterogeneity in the distribution of photosystems in these segments. Such distribution may be the consequence of the differences in the lipid or protein composition of the individual segments giving rise to the functional differences among them. However, the possibility of existence of two different kinds of fragments of thylakoids sedimenting at 40,000×g and 150,000×g and the fragment sedimenting at 90,000×g representing an intermediate fragment having some commonalities between these 40 k and 150 k fragments, cannot be ruled out. Interestingly our proteomic results had also shown that there were common proteins between 40 k and 90 k segments, 90 k and 150 k segments but there were no common proteins only between 40 k and 150 k thylakoid membrane segments (Agarwal et al. 2010).

Nevertheless, the results presented here strongly support the existence of some kind of heterogeneity in the distribution of photosynthetic supercomplexes in the thylakoids of *Synechocystis* 6803, although they appear indistinguishable at ultrastructural level. This primitive, visually indistinguishable heterogeneity may have acted as the progenitor of visible heterogeneity in terms of grana and stroma in higher plants. This “missing link” between photosynthetic bacteria and plants needs to be explored further.

Acknowledgement The authors acknowledge Dr. A. Ballal, MBD, BARC for critical reading of the manuscript.

JKS acknowledges Department of Atomic Energy, India for Raja Ramanna Fellowship.

References

Agarwal R, Ortleb S, Sainis JK, Melzer M (2009) Immunoelectron microscopy for locating Calvin cycle enzymes in the thylakoids of *Synechocystis* 6803. Mol Plant 2(1):32–42

Agarwal R, Matros A, Melzer M, Mock HP, Sainis JK (2010) Heterogeneity in thylakoid membrane proteome of *Synechocystis* 6803. J Proteomics 73:976–991

Anderson JM, Aro EM (1994) Grana stacking and protection of photosystem II in thylakoid membranes of higher plant leaves under sustained irradiance: a hypothesis. Photosynth Res 41:315–326

Andreasson E, Svensson P, Weibull C, Albertsson P (1988) Separation and characterization of stroma and grana membranes-evidence for heterogeneity in antenna size of both Photosystem I and Photosystem II. Biochim Biophys Acta 936:339–350

Armond PA, Arntzen CJ (1977) Localization and characterization of photosystem II in grana and stroma lamellae. Plant Physiol 59:398–404

Bennett A, Bogorad L (1973) Complementary chromatic adaptation in a filamentous blue green alga. J Cell Biol 58:419–435

Bryant DA, Guglielmi G, Tandeau MN, Castets AM, Cohen-Bazire G (1979) The structure of cyanobacterial phycobilisome: a model. Arch Microbiol 123(2):113–127

Dani DN, Sainis JK (2005) Isolation and characterization of a thylakoid membrane module showing partial light and dark reactions. Biochim Biophys Acta 1669:43–52

Fuhrmann E, Gathmann S, Rupprecht E, Golecki J, Schneider D (2009) Thylakoid membrane reduction affects the photosystem stoichiometry in the cyaobacteriun *Synechocystis* sp. PCC 6803. Plant Physiol 149:735–744

Hill R, Bendall F (1960) Function of the two Cytochrome components in chloroplasts: a working hypothesis. Nature 186:136–137

Holzwarth AR (1990) The functional organization of the antenna systems in higher plants and green algae as studied by time-resolved fluorescence techniques. In: Baltscheffsky M (ed) Current research in photosynthesis, Vol 2. Kluwer, Dordrecht, pp 223–230

Karukstis KK, Sauer K (1983) Fluorescence decay kinetics of chlorophyll in photosynthetic membranes. J Cell Biochem 23:131–158

Katoh T, Gantt E (1979) Photosynthetic vesicles with bound phycobilisomes from *Anabaena variabilis*. Biochim Biophys Acta 546:383–393

Keuper HJK, Sauer K (1989) Effect of photosystem II reaction center closure on nanosecond fluorescence relaxation kinetics. Photosynth Res 20:85–103

Kumazaki S, Hasegawa M, Ghoneim M, Shimizu Y, Okamoto K, Nishiyama M, Ohoka H, Terazima M (2007) A line-scanning semi confocal multi-photon fluorescence microscope with a simultaneous broadband spectral acquisition and its application to the study of the thylakoid membrane of a cyanobacteriun *Anabaena* PCC 7120. J Microscopy 228(2):240–254

Lakowicz JR (2006) Principles of fluorescence spectroscopy, 3rd edn. Springer, New York

Li Y, Zhang J, Xie J, Zhao J, Jiang L (2001) Temperature-induced decoupling of phycobilisomes from reaction centers. Biochim Biophys Acta 1504:229–234

Magde D, Berens SJ, Butler WL (1982) Picosecond fluorescence in spinach chlorolasts. Proc Soc Photo-Opt Instrum Eng 322:80–86

McCauley SW, Biltersmann E, Mueller M, Holzwarth AR (1990) Picosecond chlorophyll fluorescence from higher plants. In: Baltscheffsky M (ed) Current research in photosynthesis, Vol. 2. Kluwer, Dordrecht, pp 297–300

Mullineaux CW (2008) Phycobilisome-reaction centre interaction in cyanobacteria. Photosynth Res 95:175–182

Murata N, Sato N, Omata T, Kuwabara T (1981) Separation and characterization of thylakoid and cell envelope of the blue-green alga (cyanobacterium) *Anacystis nidulans*. Plant Cell Physiol 22:855–866

Nishiyama Y, Allakhverdiev SI, Murata NI (2005) Inhibition of the repair of Photosystem II by oxidative stress in cyanobacteria. Photosynth Res 84:1–7

Rexroth S, Mullineaux CW, Ellinger D, Sendtko E, Rögner M, Koenig F (2011) The plasma membrane of the cyanobacterium *Gloeobacter violaceus* contains segregated bioenergetic domains. Plant Cell 23:2379–2390

Rippka R, Deruelles J, Waterbury J, Herdman M, Stanier R (1979) Generic assignments, strain histories and properties of pure cultures of cyanobacteria. J Gen Microbiol 111:1–61

Santhose I, Gnanadoss J, Ramganesh S, Elumalai S (2011) Enhanced carotenoid synthesis of *Phormidium* sp. in stressed conditions. J Exp Sci 2(3):38–44

Sherman DM, Troyan TA, Sherman LA (1994) Localisation of membrane proteins in the cyanobacterium *Synechococcus* 7942: radial asymmetry in the photosynthetic complexes. Plant Physiol 138:1577–1585

Staehelin LA, Arntzen CJ (1983) Regulation of chloroplast membrane function: protein phosphorylation changes the spatial organization of membrane components. J Cell Biol 97:1327–1337

Takahashi T, Inoue-Kashino N, Ozawa SI, Takahashi Y, Kashino Y, Satoh K (2009) Photosystem II complex *in vivo* is a monomer. J Biol Chem 284(23):15598–15606

Tandeau de Marsac N, Houmard J (1988) Complementary chromatic adaptation: physiological conditions and action spectra. In: Packer L, Glazer AN (eds) Methods in enzymology: cyanobacteria, Vol 167. Academic Press Inc, San Diego, pp 318–328

Trissl HW, Wilhelm C (1993) Why do thylakoid membranes from higher plants form grana stacks? Trends Biochem Sci 18 (11):415–419

Vermaas WFJ, Timlin JA, Jones HDT, Sinclair MB, Lieman LT, Hamad SW, Melgaard DK, Haaland DM (2008) In vivo hyperspectral confocal fluorescence imaging to determine pigment localization and distribution in cyanobacterial cells. Proc Natl Acad Sci, (USA) 105(10):4050–4055

Watanabe M, Iwai M, Narikawa R, Ikeuchi M (2009) Is the photosystem II complex a monomer or a dimer? Plant Cell Physiol 50 (9):1674–1680

Wollman FA, Minai L, Nechushtai R (1999) The biogenesis and assembly of photosynthetic proteins in thylakoid membranes. Biochim Biophys Acta 1411:21–85